


Designing cellulose nanofiber surface for high density polyethylene reinforcement

Hiroyuki Yano  · Haruo Omura · Yoko Honma · Hiroaki Okumura · Hironari Sano · Fumiaki Nakatsubo

Received: 9 September 2017 / Accepted: 10 April 2018 / Published online: 18 April 2018
© The Author(s) 2018

Abstract Because of their high mechanical performance, high specific surface area, and high aspect ratio, there is a strong interest in cellulose nanofibers (CNFs) as a reinforcing material for plastics. Although three hydroxyl groups per repeating unit exposed on the surface is a unique characteristic of CNFs, an effective chemical treatment to improve the reinforcing efficiency of CNFs for hydrophobic thermoplastic resin has not yet been reported. In this study, six systematically designed aliphatic ester groups with linear, cyclic and branched structures, were incorporated on the surface of CNFs using the hydroxyl groups with a degree of substitution of 0.4. The melt compounding of the esterified CNFs and HDPE was performed at 140 °C using a twin screw extruder followed by injection molding at 160 °C and investigated the CNF dispersibility in HDPE and the CNF reinforcing efficiency in injection-molded HDPE samples. Incorporation of linear long chains results in the best dispersion of CNFs in HDPE compared with cyclic and branched chains, but the latter chains give higher reinforcing efficiencies in Young's modulus and tensile strength. Especially, the bulky t-butyl group gave the highest reinforcing efficiency. Thus, the structure of ester groups incorporated on the CNFs

very much affects on the dispersibility in HDPE, Young's modulus and tensile strength, and coefficient of thermal expansion (CTE) of the esterified CNFs-reinforced HDPE composites. Addition of pivaloylated CNFs increases the Young's modulus of HDPE from 1.20 to 3.32 GPa, and the tensile strength from 23.4 to 51.2 MPa. The CTE is 72.5 ppm/K, which is less than one-third that of the HDPE. The high reinforcing efficiency of these composites is partly explained by the formation of the double shish-kebab crystal structure during injection molding identified by the TEM observation.

Keywords Cellulose nanofibers · Surface modifications · Esterification · Nanocomposites · HDPE · Shish-kebab structure

Introduction

World plastic production is about to reach 300 million tons per year. Among the plastics, commodity plastics such as polypropylene (PP), polyethylene (PE), polyvinylchloride (PVC) and acrylonitrile butadiene styrene (ABS) account for more than 70% of plastics produced. Because of their excellent mechanical performance, as well as their high specific surface area and high aspect ratio, there is strong interest in cellulose nanofibers (CNFs) as a reinforcing material for plastics (Lindström and Christian 2014; Oksman

H. Yano (✉) · H. Omura · Y. Honma · H. Okumura · H. Sano · F. Nakatsubo
Research Institute for Sustainable Humansphere, Kyoto University, Gokashou, Uji, Kyoto 611-0011, Japan
e-mail: yano@rish.kyoto-u.ac.jp

et al. 2016). In addition, the processing temperature of these polymers is less than 200 °C, which is below the thermal deterioration temperature of CNFs (Agustin et al. 2016a, b, 2017). Therefore, CNFs are a good candidate as a reinforcing filler for these plastics, and they have attracted great interest from industry, such as automotive, home electric appliance, building materials, and packaging industries. However, all of these plastics are hydrophobic and apolar or weakly polar, whereas CNFs are strongly hydrophilic and polar because they contain three hydroxyl groups per repeating unit (anhydroglucose). Thus, improvement of the interaction between CNFs and polymers is required to realize high mechanical performance of CNFs in polymer composites.

In general, there are two approaches to improve the interaction between CNFs and polymers. One is to use compatibilizers that bridge CNFs and polymers (Ljungberg et al. 2005; Suzuki et al. 2014; Sakakibara et al. 2016). The other approach is chemical modification of the surface of CNFs (Dufresne 2012; Habibi 2014). Reinforcement of thermoplastic resin by chemically modified CNFs and cellulose nanocrystals (CNCs) has been attempted (Panaitescu et al. 2007; De Menezes et al. 2009; Lin and Dufresne 2013; Hassan et al. 2014; Huang et al. 2016). Three hydroxyl groups per repeating unit exposed on the surface is unique characteristic of CNFs and CNCs compared with other nanofillers such as carbon nanotube and carbon nanofibers and enables designing of nanofibers surface although an effective chemical treatment to improve the reinforcing efficiency of CNFs and CNCs for PP and PE has not yet been reported.

Recently, we demonstrated that alkenyl succinate anhydride treatment is effective for reinforcing high-density polyethylene (HDPE) (Sato et al. 2016). However, there is still no strategy for surface design of CNFs to attain a high mechanical reinforcing efficiency in hydrophobic polymers. In this report, six systematically designed aliphatic ester groups with linear, cyclic and branched structures, were incorporated on the surface of CNFs (Fig. 1). The esterified CNFs were melt extruded with HDPE (10 wt% CNF content) and injection molded and investigated the CNF dispersibility in HDPE and the CNF reinforcing efficiency in injection-molded HDPE samples.

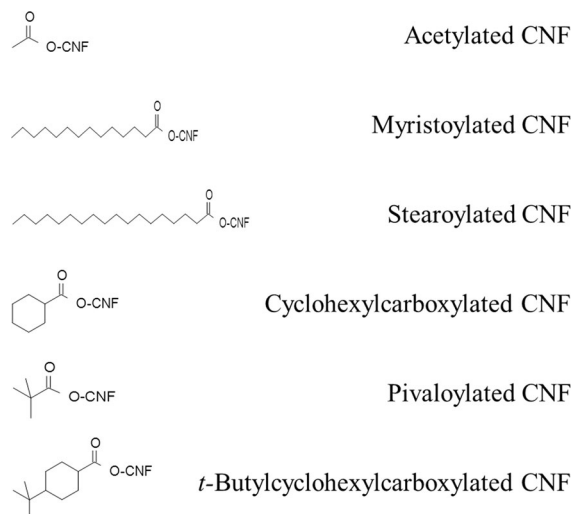


Fig. 1 Chemical structures of the incorporated chemicals

Experimental

Materials

Refiner-treated softwood bleached kraft pulp (NBKP, never-dried, α -cellulose content 85%) with 20–25 wt% solid content was supplied by Oji Holdings Corporation (Tokyo, Japan). The lignin content was 0 wt% according to Klason's method with TAPPI standard T230om-02. The Canadian standard freeness was less than 100 ml. Acetic anhydride, myristoyl chloride, stearoyl chloride, pivaloyl chloride, and cyclohexanecarbonyl chloride were purchased from Wako Pure Chemicals Industries (Osaka, Japan). 4-*t*-Butylcyclohexanecarbonyl chloride was synthesized from 4-*t*-butylcyclohexanecarboxylic acid purchased from Tokyo Kasei (Tokyo, Japan) by the general synthetic method with thionyl chloride. *N*-Methyl-2-pyrrolidone (NMP), pyridine, and other chemicals, including solvents for purification, were purchased from Wako Pure Chemicals Industries (Osaka, Japan). HDPE (Flo-Beads, HE3040, mp 130 °C, density 0.961 g/cm³) was purchased from Sumitomo Seika Co., Ltd. (Osaka, Japan). The average particle size was 11 μ m according to the supplier. All of the chemicals were used as received.

Sample preparation

Preparation of CNFs

Refiner-treated NBKP was mechanically disintegrated using a bead mill (NVM-2, AIMEX Co., Ltd., Tokyo, Japan). NBKP was diluted with distilled water to 0.75 wt%. Bead mill treatment was then performed twice at 20 °C with a rotating speed of 2000 rpm and a feed speed of 600 ml/min with 1 mm ZrO₂ beads at a packing rate of 70%. Figure 2 shows scanning electron microscopy (SEM) images of the refiner-treated NBKP and CNFs.

Surface esterification of CNFs

Surface esterification was carefully performed to avoid CNF agglomeration assured by SEM observation. A CNF slurry was filtered until it reached 20–25 wt% solid content. Wet CNFs (1 kg) and NMP (1 kg) were then mixed in a mixer (Tri-mix TX-5, 5 l, Inoue Mfg., Inc., Kanagawa, Japan) followed by evaporation of water in vacuo at 20–60 °C to give a dehydrated CNF. The CNFs (10 g) were suspended in a mixture of NMP (500 ml) and toluene (250 ml). The obtained mixture was further dehydrated by azeotropic distillation in vacuo at 70–100 °C. Acetic anhydride or acid chlorides and pyridine were added to the mixture (see Table 1). The reaction mixture was stirred under the conditions shown in Table 1, filtered to give crude esterified CNFs, which was washed twice with acetone and twice with ethanol to obtain wet esterified CNFs.

Determination of the degree of substitution

The DS value of the cellulose derivative was calculated from the area of the 1740 cm⁻¹ absorbance peak in the Fourier transform infrared (FT-IR) spectrum as described in our previous paper (Sato et al. 2016). Attenuated total reflection infrared (ATR-IR) spectra were recorded using a FT-IR spectrometer (Spectrum One, Perkin Elmer) at a resolution of 2 cm⁻¹ in the range 600–4000 cm⁻¹. All of the spectra were obtained by accumulating 16 scans and normalized using the 1315 cm⁻¹ peak of the cellulose CH₂ vibration. The DS and the area of the 1740 cm⁻¹ peak were correlated by titration of the cellulose derivatives in advance.

Preparation of CNFs composites

To prepare the composites with 10% CNF, 50 g of wet esterified CNFs containing 10 g of net CNFs, 500 ml of isopropyl alcohol, and powdered HDPE were mixed using a food mixer for 1 min to make 30 wt% CNFs. The mixture was then filtered and pressed until the solid content became ~ 30 wt%. The wet mixture was crushed and dried at 70 °C under reduced pressure using a mixer (Tri-mix TX-2, 2 l, Inoue Mfg., Inc., Kanagawa, Japan). The HDPE powder was then added to the dried mixture to make a mixture with 10 wt% CNF content. The mixture was subsequently melt extruded at 140 °C (the temperature of the barrels was set at between 110 and 140 °C) by a twin-screw extruder (KZW15-TW, Technovel Corp., Osaka, Japan) at a screw speed of 200 rpm and a feed rate of 200 g/h, and cut into pellets using a pelletizer. The screw length/diameter ratio and diameter of the extruder were 45 and 15 mm, respectively. Dumbbell

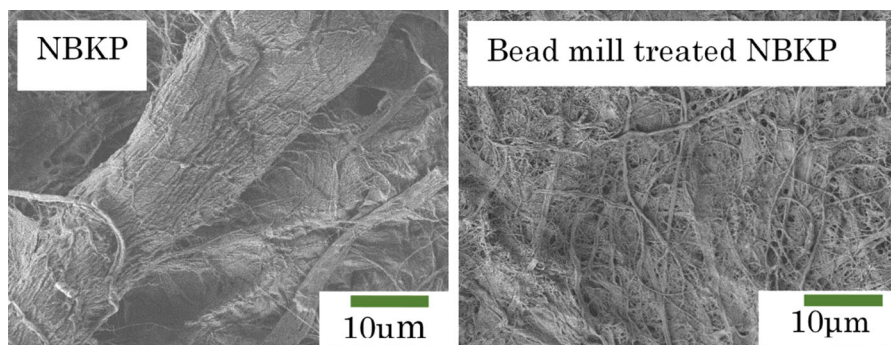


Fig. 2 SEM images of refiner treated NBKP before (left) and after (right) bead-mill treatment

Table 1 Reaction conditions for the preparation of esterified CNFs

Products	Chemicals for 10 g NBKP (61.7 mM ^a)	Temp. (°C)	Time (h)	DS	
CNF(Ac)	Acetic anhydride	240 mmol	60	5.5	0.41
	Pyridine	360 mmol			
CNF(Myristoyl)	Myristoyl chloride	100 mmol	r.t.	1	0.46
	Pyridine	220 mmol			
CNF(Stearoyl)	Stearoyl chloride	80 mmol	r.t.	2.5	0.40
	Pyridine	170 mmol			
CNF(Cyclohexanecarbonyl)	Cyclohexanecarbonyl chloride	160 mmol	r.t.	1.5	0.38
	Pyridine	210 mmol			
CNF(Pivaloyl)	Pivaloyl chloride	75 mmol	80	20	0.40
	Pyridine	110 mmol			
CNF(<i>t</i> -Butylcyclohexanecarbonyl)	<i>t</i> -Butylcyclohexanecarbonyl chloride	105 mmol	60	2	0.44
	Pyridine	210 mmol			

^aMolecular weight was tentatively regarded to be 162, anhydro glucose unit

shaped specimens were prepared from the pellets using an injection molding machine (NPX7-1F, Nissei-Plastic Industrial Co., Ltd., Nagano, Japan) at an injection temperature of 160 °C, a pressure of 100 MPa, a speed of 80 mm/s, and a mold die temperature of 40 °C. The specimens had a thickness of 1 mm, a width of 4 mm and a length of 80 mm.

The compositions of the unmodified and esterified CNF/HDPE composites samples are shown in Table 2.

Characterization

Scanning electron microscopy (SEM) observation

The original pulp and bead-mill-treated pulp slurry were filtered to make a thin wet sheet, and the sheet was then subjected to freeze drying. The freeze-dried sheets were coated with an approximately 2 nm layer of platinum using an ion sputter coater (JFC-1600, JEOL Ltd., Japan). SEM observations were performed using a JEOL JSM-6700F (field-emission scanning

electron microscope, JEOL, Ltd., Japan) under an acceleration voltage of 10 kV.

Transmittance electron microscopy (TEM) observation

Samples were embedded in epoxy resin. A Leica Ultracut UCT ultramicrotome equipped with a precision diamond knife (45°) diatome was used for specimen sectioning at room temperature. Staining was carried out in the vapor phase. The trimmed specimen embedded in epoxy resin was stained with solid RuO₄ for 20 min in a sealed glass tube. TEM observations were performed using a JEOL JEM1230 (JEOL, Ltd., Japan, accelerated voltage 120 kV).

X-ray computed tomography (X-ray CT) observation

Microcomputed tomography scanning was performed using a SKY Scan 1172 micro-CT system (Bruker Micro CT, Belgium). The specimens were cut by 4 mm along the injection direction from the center of

Table 2 Compositions of the unmodified CNF/HDPE composite and modified CNF/HDPE composite samples

	CNF (wt%)	Incorporated chemicals (wt%)	HDPE (wt%)
CNF(Ac)/HDPE	9.5%	1.0%	89.5%
CNF(Myristoyl)/HDPE	11.2%	6.6%	82.2%
CNF(Stearoyl)/HDPE	10.3%	7.4%	82.3%
CNF(Cyclohexanecarbonyl)/HDPE	10.6%	3.5%	85.9%
CNF(Pivaloyl)/HDPE	11.2%	2.6%	86.2%
CNF(<i>t</i> -BuC)	10.4%	4.7%	84.9%
Unmodified CNF/HDPE	10.7%	–	89.3%

the dumbbell shaped samples. The observations were performed for the cross-section of molded samples with 1 mm thickness and 4 mm width. The area of the specimens used for the evaluation was $600 \mu\text{m}^2 \times 200 \mu\text{m}$ and the resolution was 700 nm.

Thermogravimetric analysis (TGA)

The thermal durability and cellulose content of the samples were determined by TGA based on the weight change due to heating. TGA was performed on a Q-50 thermogravimetric analyzer (TA Instruments, USA) under a nitrogen atmosphere (60 ml/min) at a heating rate of 10 °C/min.

Measurement of viscoelasticity

The temperature dependences of the shear moduli (G') of the composites were measured between 110–160 °C with a rheometer (AR-G2, TA Instruments, USA) using parallel plates with an 8 mm diameter geometry and the forced vibration method in shear mode under a nitrogen atmosphere with a frequency of 1 Hz, 0.1% strain, and a heating rate of 1 °C/min.

Measurement of mechanical properties

The tensile modulus and strength of the injection-molded composites were measured using a universal testing machine (Model 3655, Instron Corp., USA) with a crosshead speed of 10 mm/min at 23 °C. The load cell of the machine was 5 kN. The elongation was measured using a video camera. Five specimens were tested, and the reported values are averages of these five specimens.

Measurement of coefficients of thermal expansion (CTEs)

The CTEs were measured by a thermomechanical analyzer (TMA/SS6100, SII Nanotechnology Inc., Japan). The specimens were 25 mm long, 3 mm wide, and 1 mm thick with a 20 mm span. The measurements were performed three times during elongation with a heating rate of 5 °C/min in a nitrogen atmosphere at a load of 3 g. The CTE values were determined as the mean values in the range 50–100 °C in the second run.

Results and discussion

Preparation of aliphatic esters

The chemical structures and their abbreviations of these six aliphatic CNF-esters are shown in Fig. 1, i.e. three linear acyclic: acetyl (C2), myristoyl (C14) and stearoyl (C18), two cyclic: cyclohexanecarboxyl (C7) and t-butylcyclohexanecarboxyl (C11) without and with branched structures, respectively, one branched esters: pivaloyl (C5).

The esterification was carried out under the general reaction conditions shown in Table 1 to afford the products with DS of around 0.4, although the introduction of pivaloyl group took longer reaction time and higher temperature because its steric hindrance. Here, we determined to be the expected DS around 0.4, because the esterification giving the DS less than 0.55 did not affect to the crystallinity of the original CNF as described in our previous paper (Sato et al. 2016). That is, the esterification is limited in only on the surface of the CNFs.

Thermal durability of the esterified CNFs

The melt compounding of the esterified CNFs and HDPE was performed at 140 °C using a twin screw extruder followed by injection molding at 160 °C. In these processes, the CNFs are subjected to high shear stress. Thus, thermal deterioration of the CNFs during the melt compounding and injection molding process is a great concern because damage to the CNFs would affect their reinforcing ability. Especially, elimination of the incorporated ester groups from the esterified CNFs under such high temperature may be serious (Agustin et al. 2016a). Even if it results in 1% weight loss, the evolved gas could affect the micro and nanostructures of the molded samples, resulting in poor mechanical properties. Hence, the temperatures resulting in 1 and 5% weight loss of the esterified CNFs were determined as summarized in Table 3 along with the peak temperatures of the differential curves of TGA.

As shown in the table, the 1% weight loss temperatures for all six esterified CNFs are higher than that of the unmodified CNF, and the temperatures are in the range 270–280 °C. In particular, the CNF(Cyc) and CNF(Piv) exhibit high 1% weight loss temperature of 282 and 285 °C, respectively. These

Table 3 1 and 5% weight loss temperatures (1% WL temp. and 5% WL temp.) and the temperatures at the maximum weight loss rate (Peak temp.) of unmodified CNF and its esters

	1% WL temp. (°C)	5% WL temp. (°C)	Peak temp. (°C)
CNF(Ac)	273	309	367
CNF(Myr)	272	310	371
CNF(Ste)	278	314	377
CNF(Cyc)	285	321	366
CNF(Piv)	282	319	378
CNF(<i>t</i> -BuC)	277	306	372
Unmodified CNF	258	300	353

temperatures are 27 and 24 °C higher than that of the unmodified CNF.

As reported by Agustin et al. (2016b) from the pyrolysis products, it can be deduced that removal of esters groups on the surface of CNFs can take place in two ways: the direct cleavage of the ester bonds from the cellulose chain to release the equivalent carboxylic acids; and the possible condensation reaction between adjacent two esters on the surface of CNFs to produce symmetrical ketones. It seems that straight chain esters were removed mainly by condensation reaction of the chain esters. On the other hand, bulky esters of CNF (Cyc) and CNF (Piv) were removed only by direct ester bond cleavage by steric hindrance effect of bulky esters. The lower onset of thermal degradation displayed by CNFs esters with straight-chain carbon esters than those of bulky esters is attributed to the possible lower energy to deprotect by condensation reaction than direct ester bond cleavage.

The 5% weight loss temperatures of the esterified CNFs are all higher than that of the unmodified CNF, and they are all above 300 °C. Thus, the esterification used in this study is great useful for the protection against the thermal deterioration and disengagement during melt compounding and injection molding.

Dispersibility of CNFs in HDPE and the interaction between CNFs and HDPE at the melted condition

The dispersibility of esterified CNFs in HDPE and the interaction between CNFs and HDPE at the melted condition were evaluated by X-ray CT (resolution: 700 nm) and by the G' value of the CNFs/HDPE composite at the melted condition obtained by dynamic mechanical analysis, respectively.

The X-ray CT images of esterified CNFs-reinforced HDPE are shown in Fig. 3 along with the images of

unmodified CNF-reinforced HDPE and neat HDPE. The X-ray CT images displays density distribution detected by X-ray intensity attenuation. The resolution of 700 nm in this work is insufficient to allow a detailed evaluation of the nanocomposite materials, but the 3D images do offer useful information about agglomerations of cellulose fibers in the low density polymers such as HDPE (Sato et al. 2016; Sakakibara et al. 2016) and acrylic resin (Yano et al. 2014). In this study, the cellulose with a density of 1.6 g/cm³ and HDPE with a density of 0.92 g/cm³ is represented by white bright color and blue color, respectively. The bright points observed in the CNF-reinforced HDPE indicate the CNF aggregates with the size over 700 nm.

The agglomeration to produce the aggregates seems to mostly have occurred during melt compounding and injection molding, because NBKP fibrillated to nanofibers as shown in Fig. 2 was carefully esterified to avoid CNF agglomeration. The agglomeration can be attributed to the difference in the interaction between the functional groups incorporated on the surface of the CNF and HDPE.

The size and frequency of the CNF aggregates differ among the composites. As shown in Fig. 3, many bright points were observed especially in unmodified-CNF-and also CNF(Ac, C2)-reinforced HDPE, but did not in CNF(Myr, C14) and CNF(Ste, C18)-reinforced HDPE, indicating that the incorporation of acyclic long alkyl chain on the surface of CNF enable the CNFs to well disperse in HDPE. This is because that the long alkyl chains resembling the repeating unit of PE thickly cover the surface of CNFs.

The CNF(Cyc, C7) with the different carbon skeleton from the long alkyl chain is suggested not to disperse well in HDPE. Actually, the CNF(Cyc, C7)-HDPE composite gave a many bright spots, but interestingly the spots markedly disappeared in the

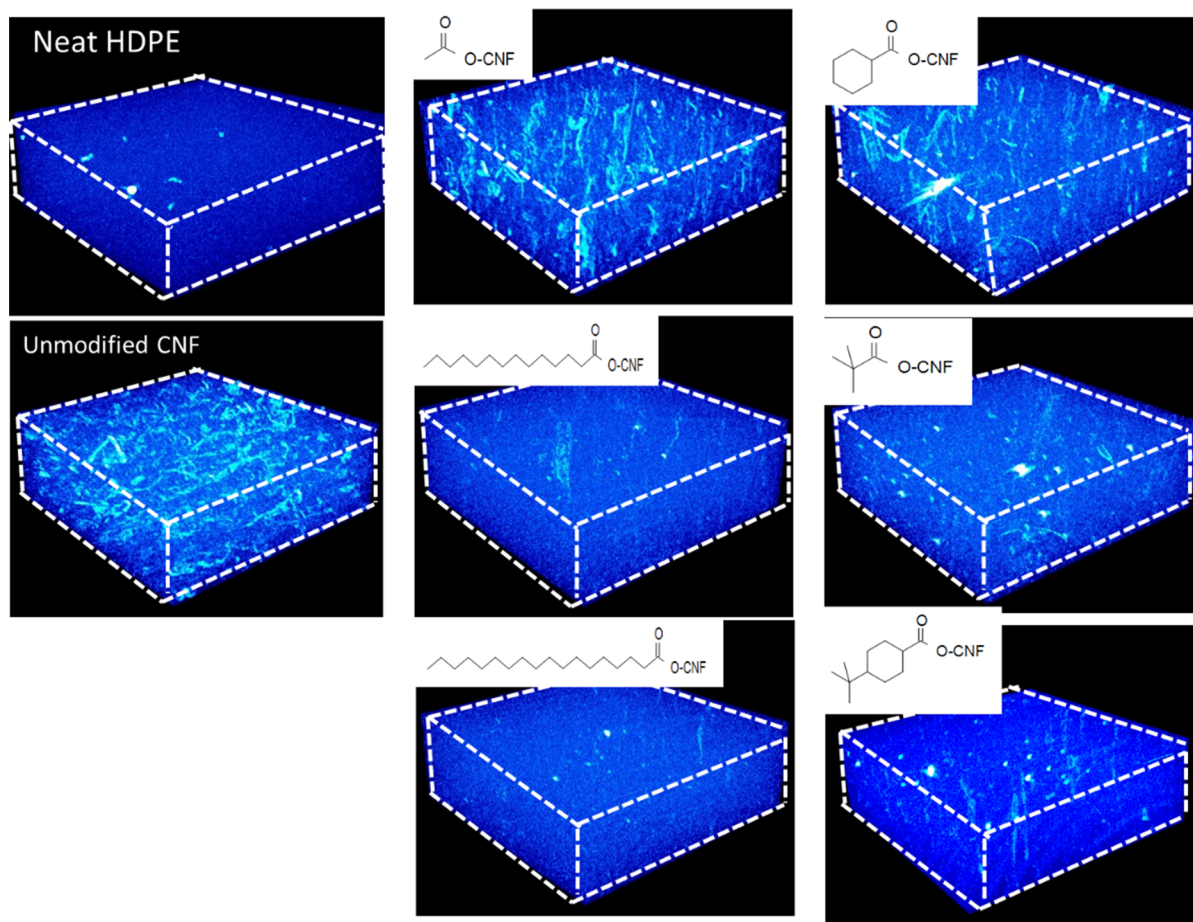


Fig. 3 X-ray CT images of injection-molded HDPE and the HDPE composites (resolution 700 nm, the samples were injected from the bottom to the top)

case of the CNF(t-BuCyc, C11), indicating that the additional incorporation of bulky t-butyl group enables to improve its dispersibility.

Finally, the CNF (Piv, C5)-HDPE composite which is reinforced with CNF having only the simplest bulky t-butyl group gave comparable X-ray CT image with that of the CNF(t-BuCyc, C11). Thus, we found that terminal bulky t-butyl group play an important role in improving the dispersity in HDPE, in spite of the completely different carbon skeleton for HDPE.

Temperature dependence of the shear modulus (G') of the esterified CNFs/HDPE composites are shown in Fig. 4 along with the unmodified CNF/HDPE composite and neat HDPE. The results are summarized in Table 4.

The CTE values were determined as the mean values in the range 50–100 °C in the second run. The

numbers in parentheses indicate the standard deviations.

The G' value is generally used as an index for judging the interaction between the filler and polymer matrix. That is, larger G' value under melted state indicates higher interaction between them at melted state. The differences in the G' values can be attributed to the differences in the contact areas of the CNFs and HDPE (dispersibility of the CNFs) and the chemical interactions between the CNF surfaces and HDPE.

As shown in Fig. 4, the G' value of HDPE decreases at around 120 °C and becomes 0.0036 MPa at 140 °C owing to melting. When untreated CNFs were added, the G' value at 140 °C is about 20 times higher than that of HDPE and maintains an almost constant value up to 160 °C. This constant G' value can be explained by the formation of the mechanical network of CNFs

Fig. 4 Temperature dependency of the shear modulus of HDPE, the unmodified CNF/HDPE composite, and the modified CNF/HDPE composites (1 °C/min, 160 → 110 °C, 0.1% strain, 1 Hz)

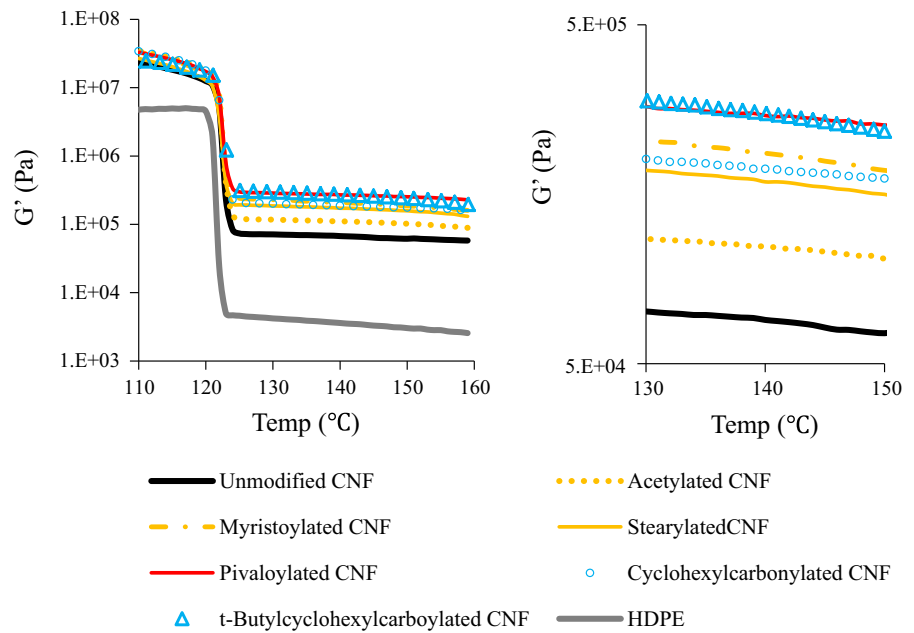


Table 4 Shear modulus (G') at 140 °C, Young's modulus, tensile strength, and CTE of HDPE, the unmodified CNF/HDPE composite, and the modified CNF/HDPE composites

	G' ($\times 10^3$ Pa) @140C	Young's modulus (GPa)	Tensile strength (MPa)	CTE (ppm/k)
CNF(Ac)/HDPE	111.0	2.25 (0.10)	39.6 (0.42)	163.1
CNF(Myrr)/HDPE	209.0	2.60 (0.02)	50.4 (0.80)	93.5
CNF(Ste)/HDPE	172.0	2.42 (0.11)	48.1 (0.44)	101.6
CNF(Cyc)/HDPE	188.0	2.78 (0.11)	47.2 (0.22)	107.5
CNF(Piv)/HDPE	270.0	3.32 (0.04)	51.2 (0.89)	72.5
CNF(<i>t</i> -BuC)/HDPE	273.6	2.96 (0.04)	48.2 (0.06)	101.3
Unmodified CNF/HDPE	67.3	2.08 (0.41)	34.2 (0.10)	136.4
HDPE	3.6	1.20 (0.16)	23.4 (0.23)	244.4

whose Young's modulus does not change until 200 °C (Nishino et al. 2007; Nakagaito et al. 2009).

The G' values at the melted condition are significantly different among the esterified CNFs. The combination of unmodified CNF and HDPE gives the lowest G' value at 140 °C, followed by CNF(Ac)/HDPE. Unmodified CNF and CNF(Ac) result in many aggregates in the composite, as shown in X-ray CT, indicating a poor affinity with HDPE. On the other hand, CNF(Cyc) which also exhibit poor dispersibility comparable with that of CNF(Ac) (Fig. 3), exhibit a similar G' value to those of CNF(Myrr) and CNF(Ste) at the melting condition, which show good

dispersibility in HDPE. Judging from G' at the melted condition and X-ray CT analysis the rigid ring structure incorporated on the CNFs seems to restrain movement of PE molecule chains more effectively than the flexible long alkyl chain. Introduction of a tertiary butyl group to cyclohexane ring further increases the G' . This can be explained by the improved dispersibility of the CNFs, as described above.

An interesting result is observed for CNF(Piv)-HDPE composite. The CNF(Piv) has poor dispersibility in HDPE compare to CNF(Myrr) and CNF(Ste) with long alkyl chain as shown in Fig. 3, however, the G'

value at 140 °C is highest in all esterified CNFs-reinforced HDPE composites. Although the mechanism should be further investigated, it is worth noting that the interaction between esterified CNFs and HDPE cannot be explained by the only the dispersibility of the CNFs in the matrix HDPE.

Mechanical properties and thermal stability of esterified CNF-reinforced HDPE

The Young's modulus, and tensile strength of the injection molded samples are compared in Table 4. The typical stress–strain curves in tension and the thermal expansion curves are shown in Fig. 5. The densities of the samples are in the range 0.96–1.02 g/cm³. The cellulose content was fixed at 10 wt% to compare the effect of surface modification of the CNFs.

Addition of acetylated CNFs increases the Young's modulus of HDPE from 1.20 to 2.25 GPa, and the tensile strength from 23.4 to 39.6 MPa. The effect of acetylation is not significant when it is compared with untreated-CNF-reinforced HDPE. As shown in Figs. 3 and 4, CNF(Ac) does not disperse well in HDPE and the G' value at the melting condition is low. This poor affinity of CNF(Ac) for HDPE is the main reason for the low reinforcing efficiency. Increasing the length of the alkyl chain improves the mechanical reinforcement efficiency of CNFs. The CNF(Myristoyl) attains a Young's modulus of 2.60 GPa, which is

approximately 2 times that of neat HDPE, and a tensile strength of 50.4 MPa. The increase of the affinity with the increase of the length of the alkyl chain results in good dispersion of CNFs and thus increases the interphase area between the CNFs and HDPE, contributing to the high reinforcing efficiency of HDPE. However, further increasing the alkyl chain length, such as CNF(Ste), decreases the Young's modulus of the composite, although stearylation achieves the best dispersibility of CNFs. It is possible that the longer chain length plasticizes the HDPE because of the flexible and bulky functional groups.

Introduction of rigid functional groups was then evaluated using cyclic fatty acids to compare with linear fatty acids. CNF(Cyc) increases the Young's modulus of HDPE to 2.78 GPa, and interestingly higher than that of CNF(Myristoyl)-reinforced HDPE. As shown in Fig. 3, the CNF(Cyc) shows poor dispersibility in HDPE, although they have a similar G' value to CNF(Myristoyl) at the melting condition. Thus, rigid cyclic fatty acid structures effectively inhibit deformation of HDPE molecules and achieve higher reinforcing efficiency than linear fatty acid structures irrespective of their poor dispersibility. The effect of addition of a tertiary butyl group to the cyclic fatty acid structure was then investigated. Although introduction of a tertiary butyl group to cyclohexane improves the dispersibility of CNFs in HDPE, the degree of the improvement in the mechanical properties is relatively small.

Fig. 5 Typical stress–strain curves and thermal expansion curves for HDPE, the unmodified CNF/HDPE composite, and the modified CNF/HDPE composites

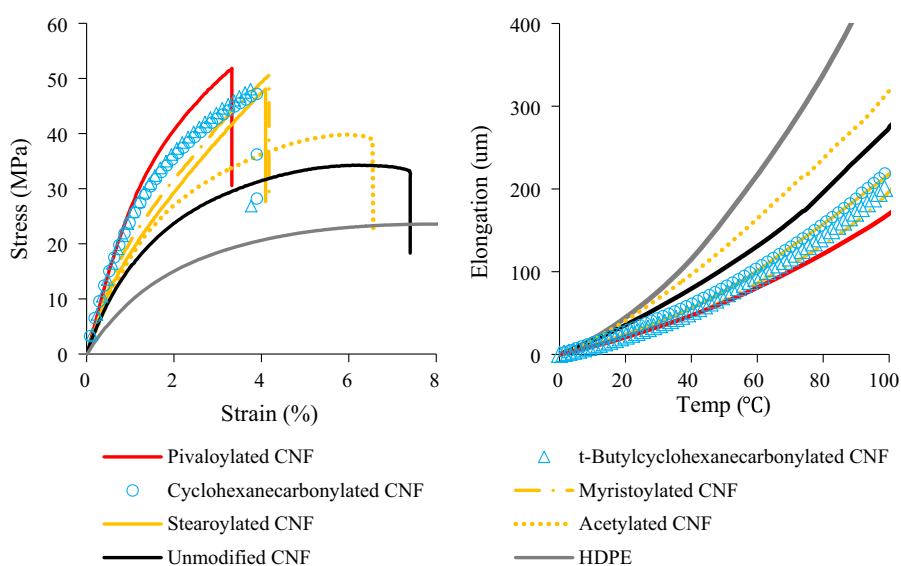
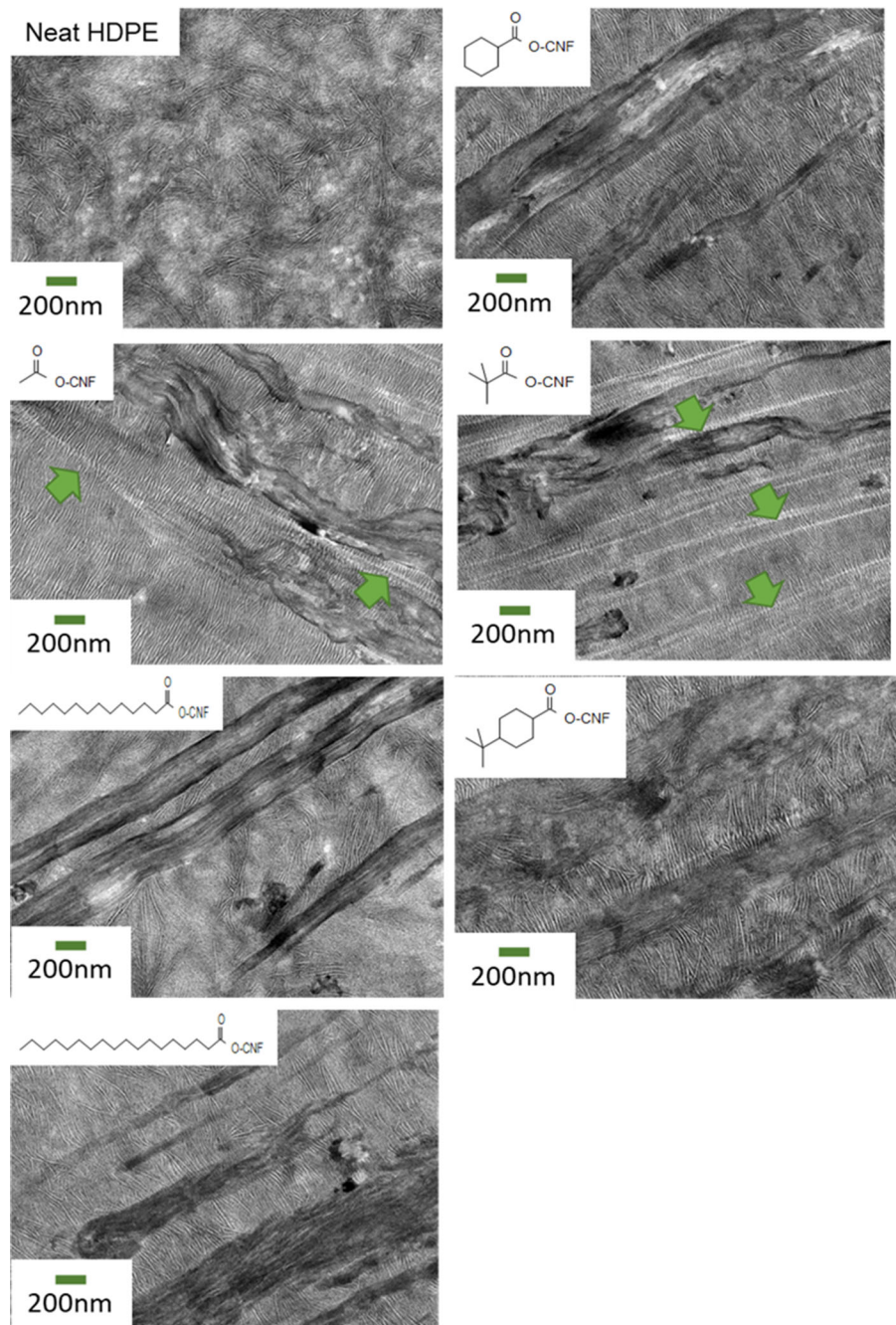


Fig. 6 TEM images of HDPE and the modified CNF/HDPE composites. The green arrows indicate HDPE “shish” structures



An interesting reinforcing efficiency was obtained with CNF(Piv). CNF(Piv)-reinforced HDPE exhibited the highest Young's modulus of 3.32 GPa and tensile strength of 51.2 MPa. Taking into account that the Young's modulus of neat HDPE is 1.20 GPa, the reinforcing efficiency of CNF(Piv) is two times higher

than that of CNF(Ste), which exhibited the best dispersibility in HDPE. The dispersibility of CNF(Piv) is not matched by CNF(My) and CNF(Ste). Nevertheless, CNF(Piv) gives the highest G' value at the melting condition and the highest Young's modulus among the modified CNFs.

The CTEs calculated between 50 and 100 °C are shown in Table 4. In general, there is a relationship between the degree of increase of the rigidity and the degree of decrease of thermal expansion in CNF composites (Nakagaito and Yano 2008). The decrease in the CTE is pronounced in the composites reinforced with CNFs incorporating long alkyl chains, such as myristoyl and stearoyl groups. In addition, despite its poor dispersibility, CNF(Cyc) exhibited a similar reinforcing efficiency to CNF(Myrist). As observed in the Young's modulus, the highest reinforcing efficiency in the CTE is attained with CNF(Piv). The CTE is 72.5 ppm/K, which is less than one-third that of the neat resin.

TEM observation of injection-molded CNF-reinforced HDPE

The highest reinforcing efficiency in the Young's modulus and CTE attained with the CNF(Piv) indicates that a chemical structure that strongly restrains HDPE molecules at the melting condition gives a high reinforcing efficiency after injection molding. Analysis of the mechanism of the high reinforcing efficiency would give insight into design of chemical structures incorporated on CNFs for polymer reinforcement. Hence, TEM observation of injection-molded CNF-reinforced HDPE was performed (Fig. 6). The TEM image of CNF(Piv)-reinforced HDPE reveals an interesting polymer structure, that is, a CNF "shish"/HDPE "kebab" structure and a HDPE "shish"/HDPE "kebab" structure. The white lines indicated by green arrows are HDPE "shish" structures. The flow-induced HDPE shish structure is a semicrystalline extended polymer chain (Mitsuhashi 1964; Pennings and Kiel 1965; kimata et al. 2007), and the crystal of HDPE is known to exhibit incredibly high elastic modulus such as 240GPa (Sakurada et al. 1966). This HDPE "shish"/HDPE "kebab" structure is slightly observed in CNF(Ac)-reinforced HDPE and is not clearly observed in CNF(Cyc)-reinforced HDPE and CNF(t-BuCyc)-reinforced HDPE. Furthermore, for the CNF(Myrist), irregular growth of HDPE kebab structures is observed. The high reinforcing efficiency of CNF(Piv) can be partially attributed to generation of extended HDPE chain structures as well as a well-ordered folded HDPE crystal structure. The kebab structures disappeared when the composite was melted and cooled. This indicates that chemically modified

CNFs do not act as a nucleating agent. Because CNF(Piv)-reinforced HDPE exhibits a high G' value at the melted condition, it seems that the shear flow of the melted polymer in the injection molding die is trapped by the CNF network and polymer chains are subjected to high shear stress because of the surface chemical structure of the CNFs, which generate a CNF shish/HDPE kebab structure as well as a HDPE shish/HDPE kebab structure. It is worthy to note that surface modification of CNFs controls the crystal structure of HDPE during injection molding.

Conclusions

Six systematically designed aliphatic ester groups with linear, cyclic and branched were incorporated on the surface of CNFs. The esterified CNFs were melt-extruded with HDPE and injection molded. The incorporation of long linear chain such as stearoyl results in the best dispersion of CNFs in HDPE, however, the highest reinforcing efficiency in tensile modulus, tensile strength and linear thermal expansion was attained by the incorporation of branched chain such as pivaloyl. The highest G' value at melted condition were demonstrated by pivaloylated CNFs despite of poor dispersibility. Since the flow-induced shish-kebab structures were clearly observed by TEM images after injection molding of pivaloylated CNFs reinforced HDPE composite, the incorporation of branched structure on the surface of CNFs seems to be effective to generate extended polymer super-structure as well as well-ordered folded HDPE crystal structures by flow-induced molding. Although further investigation is required, the structural control of HDPE by surface modification of CNFs would open the door for next-generation nanocomposites.

Acknowledgments This work was supported by the New Energy and Industrial Technology Development Organization (NEDO) P09010, Japan and Grant-in-Aid for challenging Exploratory Research, 15K13787, Japan.

Open Access This article is distributed under the terms of the Creative Commons Attribution 4.0 International License (<http://creativecommons.org/licenses/by/4.0/>), which permits unrestricted use, distribution, and reproduction in any medium, provided you give appropriate credit to the original author(s) and the source, provide a link to the Creative Commons license, and indicate if changes were made.

References

- Agustin MB, Nakatsubo F, Yano H (2016a) The thermal stability of nanocellulose and its acetates with different degree of polymerization. *Cellulose* 23:451–464
- Agustin MB, Nakatsubo F, Yano H (2016b) Products of low-temperature pyrolysis of nanocellulose esters and implications for the mechanism of thermal stabilization. *Cellulose* 23:2887–2903
- Agustin MB, Nakatsubo F, Yano H (2017) Improved resistance of chemically-modified nanocellulose against thermally-induced depolymerization. *Carbohydr Polym* 164:1–7
- De Menezes AJ, Siqueira G, Curvelo AAS, Dufresne A (2009) Extrusion and characterization of functionalized cellulose whiskers reinforced polyethylene nanocomposites. *Polymer* 50:552–4563
- Dufresne A (2012) Nanocellulose: from nature to high performance tailored materials. *Walter De Gruyter, Berlin*, pp 164–191
- Habibi Y (2014) Key advances in the chemical modification of nanocelluloses. *Chem Soc Rev* 43:1519–1542
- Hassan ML, Mathew AP, Hassan EA, Fadel SM, Oksman K (2014) Improving cellulose/polypropylene nanocomposites properties with chemical modified bagasse nanofibers and maleated polypropylene. *J Reinf Plast Compos* 33:26–36
- Huang P, Zhao Y, Kuga S, Wu M, Huang Y (2016) A versatile method for producing functionalized cellulose nanofibers and their application. *Nanoscale* 8:3753–3759
- Kimata S, Sakurai T, Nozue Y, Kasahara T, Yamaguchi N, Karino T, Shibayama M, Kornfield JA (2007) Molecular basis of the shish-kebab morphology in polymer crystallization. *Science* 316:1014–1017
- Lin N, Dufresne A (2013) Physical and/or chemical compatibilization of extruded cellulose nanocrystal reinforced polystyrene nanocomposites. *Macromolecules* 46:5570–5583
- Lindström T, Christian A (2014) Market and technical challenges and opportunities in the area of innovative new materials and composites based on nanocellulosics. *Scand J For Res* 29(4):345–351
- Ljungberg N, Bonini C, Bortolussi F, Boisson C, Heux L, Cavallé JY (2005) New nanocomposite materials reinforced with cellulose whiskers in atactic polypropylene: effect of surface and dispersion characteristics. *Biomacromolecules* 6:2732–2739
- Mitsuhashi S (1964) On the crystalline textures of polyethylene grown under rotational flow in xylene solution. *Bull Text Res Inst* 66:1–9
- Nakagaito AN, Yano H (2008) The effect of fiber content on the mechanical and thermal expansion properties of biocomposites based on microfibrillated cellulose. *Cellulose* 15:555–559
- Nakagaito AN, Fujimura A, Sakai T, Hama Y, Yano H (2009) Production of microfibrillated cellulose (MFC)-reinforced polylactic acid (PLA) nanocomposites from sheets obtained by a papermaking-like process. *Compos Sci Technol* 69:1293–1297
- Nishino T, Kotera M, Kimoto M (2007) Temperature dependence of the elastic modulus of the crystalline regions of celluloses. In: *Proceedings of 2nd international cellulose conference*, p 125
- Oksman K, Aitomäki Y, Mathew AP, Siqueira G, Zhou Q, Butylina S, Tanpichai S, Zhou X, Hooshmandet S (2016) Review of the recent developments in cellulose nanocomposite processing. *Composites A* 83:2–18
- Panaitescu DM, Donescu D, Bercu C, Vuluga DM, Iorga M, Ghiurea M (2007) Polymer composites with cellulose microfibrils. *Polym Eng Sci* 47:1228–1234
- Pennings AJ, Kiel AM (1965) Fractionation of polymers by crystallization from solution, on the morphology of fibrillar polyethylene crystals grown in solution. *Kolloid Z Z Polym* 205:160–162
- Sakakibara K, Yano H, Tsujii Y (2016) Surface engineering of cellulose nanofiber by adsorption of diblock copolymer dispersant for green nanocomposites materials. *ACS Appl Mater Interfaces* 8:24893–24900
- Sakurada I, Ito T, Nakamae K (1966) Elastic moduli of the crystal lattices of polymers. *J Polym Sci Part C* 15:75–91
- Sato A, Kabusaki D, Okumura H, Nakatani T, Nakatsubo F, Yano H (2016) Surface modification of cellulose nanofibers with alkenyl succinic anhydride for high-density polyethylene reinforcement. *Compos Part A* 83:72–79
- Suzuki K, Sato A, Okumura H, Hashimoto T, Nakagaito AN, Yano H (2014) Novel high-strength, micro fibrillated cellulose-reinforced polypropylene composites using a cationic polymer as compatibilizer. *Cellulose* 21:507–518
- Yano H, Sasaki Md, Iftekhar S, Abe K, Date T (2014) Wood pulp-based optically transparent film: a paradigm from nanofibers to nanostructured fibers. *Adv Opt Mater* 2:231–234